

# Preparation of walnut shell-based activated carbon and its properties for simultaneous removal of H<sub>2</sub>S, COS and CS<sub>2</sub> from yellow phosphorus tail gas at low temperature

Kai Li<sup>1</sup> · Haotian Ruan<sup>1</sup> · Ping Ning<sup>1</sup> · Chi Wang<sup>2</sup> · Xin Sun<sup>1</sup> · Xin Song<sup>1</sup> · Shuang Han<sup>1</sup>

Received: 5 May 2017 / Accepted: 4 October 2017 / Published online: 26 October 2017  
© Springer Science+Business Media B.V. 2017

**Abstract** Walnut shell-based activated carbon (WSBAC) was prepared used to simultaneously remove H<sub>2</sub>S, COS and CS<sub>2</sub> from yellow phosphorus tail gas and closed carbide furnace tail gas. The influences of different preparation conditions (carbonization temperature, activating agent species, activating agent content, activation temperature) on the simultaneous removal efficiency of H<sub>2</sub>S, COS and CS<sub>2</sub> were investigated. The results showed that the WSBAC carbonized at 600 °C, then activated with 0.5 times KOH at 700 °C had the highest sulfur capacity (52.67 mgS/g<sub>WSBAC</sub>). The structure and surface properties of the catalysts were characterized by Brunauer–Emmett–Teller (BET) method, and the results showed that the high BET surface area (484.26 m<sup>2</sup>/g), high micropore volume (0.261 cm<sup>3</sup>/g) and more pore sizes of 0.3–1.8 nm were conducive to the simultaneous removal of H<sub>2</sub>S, COS and CS<sub>2</sub>. X-ray photoelectron spectroscopy results showed that the most of products on the exhausted WSBAC were S/SO<sub>4</sub><sup>2-</sup> species which accumulated on the WSBAC's surface and had a negative effect on the adsorption activity.

**Keywords** Walnut shell-based activated carbon (WSBAC) · Simultaneous removal of H<sub>2</sub>S, COS and CS<sub>2</sub> · Yellow phosphorus tail gas · Closed carbide furnace tail gas

---

✉ Chi Wang  
wangchikg@163.com

<sup>1</sup> Faculty of Environmental Science and Engineering, Kunming University of Science and Technology, Kunming 650500, China

<sup>2</sup> Faculty of Chemical Engineering, Kunming University of Science and Technology, Kunming 650500, China

## Introduction

Yellow phosphorus tail gas and closed carbide furnace tail gas contain a large number of CO (85 ~ 95%), and a small amount of H<sub>2</sub>S (400–600 ppm), COS (300–600 ppm), CS<sub>2</sub> (20–60 ppm), etc. CO is an important chemical raw material for one carbon industry. H<sub>2</sub>S, COS and CS<sub>2</sub> can pollute the environment and poison the catalyst [1, 2]. Therefore, it is valuable to remove H<sub>2</sub>S, COS and CS<sub>2</sub>. So far, the common removal methods include adsorption (for H<sub>2</sub>S removal), catalytic oxidation (for H<sub>2</sub>S removal) and catalytic hydrolysis (for COS and CS<sub>2</sub> removal) [3–7]. As a kind of sorbent/catalyst, carbon materials have been widely used in the industry. However, the simultaneous removal of three gaseous pollutants is a challenge for researchers, and there are few reports about the application of carbon materials for simultaneous removal of H<sub>2</sub>S, COS and CS<sub>2</sub> from yellow phosphorus tail gas and closed carbide furnace tail gas.

Biological activated carbon comes from the thermal degradation of organic materials such as crop residues, forest residues, wood, manure, and other materials [8, 9]. Biologically activated carbon has an excellent pore structure and oxygen functional groups [10]. These advantages make biologically activated carbon a good application prospect in the field of environmental catalysts. In some fields, scientists have carried out research on the application of biologically activated carbon [11–14]. Yu et al. [15] prepared biologically activated carbon from walnut shells, which showed a high surface area (1434 m<sup>2</sup>/g) and rich microporous structure. Stephan et al. prepared walnut shell-based activated carbon, which showed high adsorption ability [16]. Song et al. and Li et al. prepared walnut shell-based activated carbon (WSBAC) as a catalyst for the removal of COS and CS<sub>2</sub>, and it showed high removal efficiency [17, 18]. In the Yunnan province of China, there is plenty of biomass material, including walnut shells, cigarette rods, straw, etc. In particular, thousands of tons of walnut shells are burned or disposed as landfill which not only pollutes the environment but also wastes resources. Thus, as a kind of new biologically activated carbon, WSBAC can be used to control the gaseous pollution of the chemical industry in Yunnan province.

In this study, a series of WSBAC materials were prepared and used for the simultaneous removal of H<sub>2</sub>S, COS and CS<sub>2</sub> from yellow phosphorus tail gas and closed carbide furnace tail gas at low temperature (< 100 °C). The influences of carbonization temperature, activating agent species, activating agent contents and activation temperature on the simultaneous removal efficiency were investigated. The Brunauer–Emmett–Teller (BET) method was used to analyze the structure and surface properties of the WSBAC samples with different preparation conditions. XPS was used to analyze the deactivation process on the simultaneous removal of H<sub>2</sub>S, COS and CS<sub>2</sub> over WSBAC.

## Materials and methods

### Materials preparation

In this study, walnut shells from Yunnan province were used as the raw material of WSBAC. Firstly, the walnut shells were washed with distilled water 2 times and

then dried at 100 °C in a drying oven. Secondly, the shells were broken to 4-mesh size, and then carbonized at 400–800 °C for 1 h under a nitrogen environment in the pipe furnace. The carbonized material was ground and sieved to 40- to 60-mesh size. Then, it was activated with an activator ( $\text{H}_3\text{PO}_4$ , KOH,  $\text{ZnCl}_2$ ,  $\text{K}_2\text{CO}_3$ ) at 600–900 °C for 1 h under a nitrogen environment in the pipe furnace. Next, the WSBAC was washed with 0.1 mol/L  $\text{HNO}_3$  1–2 times, and then washed with distilled water to a constant pH ( $\text{pH} = 7$ ) to remove the ash and the activating agent. Finally, it was dried at 100 °C in the drying oven for 6 h.

## Materials characterization

Nitrogen adsorption–desorption isotherms were measured using a Quantachrome 2000 surface area analyzer. The samples were initially out-gassed at 393 K for 24 h. The HK method was used to calculate the pore size distribution of the WSBAC. The BET method was used to calculate the surface area. XPS (ESCALAB 250) analysis was performed using Al K $\alpha$  radiation equipped with an Al target (200 W).

## Desulphurization test

As shown in Fig. 1, desulfurization tests were performed in a fixed-bed quartz reactor (3 mm inside diameter, 140 mm length) under atmospheric pressure.  $\text{H}_2\text{S}$ , COS and  $\text{CS}_2$  from gas cylinders (1%  $\text{H}_2\text{S}$  in  $\text{N}_2$ ; 1% COS in  $\text{N}_2$ ; 0.3%  $\text{CS}_2$  in  $\text{N}_2$ ) were diluted with  $\text{N}_2$  (99.99%) to the required concentration ( $\text{H}_2\text{S}$ : 500 ppm; COS: 400 ppm;  $\text{CS}_2$ : 40 ppm). Calibrated mass flow controllers were used to control the overall flow rate (50 mL/min), and the overall gas hourly space velocity (GHSV) of

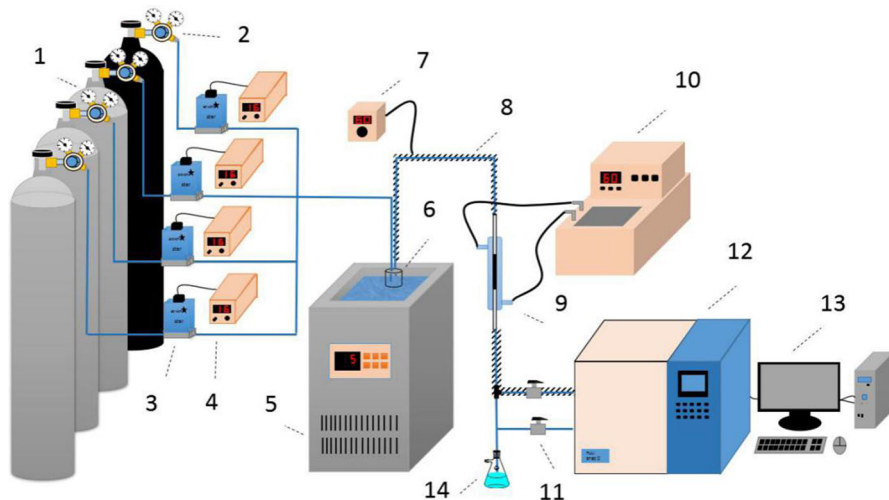


**Fig. 1** Schematic diagram of the apparatus for  $\text{H}_2\text{S}$ , COS,  $\text{CS}_2$  simultaneous removal: 1  $\text{N}_2$ ,  $\text{H}_2\text{S}$ , COS and  $\text{CS}_2$ ; 2 reducing valve; 3 mass flowmeter; 4 display; 5 low temperature thermostat; 6 water saturator; 7 temperature controller; 8 heater band; 9 reactor; 10 digital circulating water bath; 11 valve; 12 GC; 13 computer

the reaction mixture was standardized at  $4000 \text{ h}^{-1}$ . The water came from a saturator system, and the relative humidity (RH) was used to express the  $\text{H}_2\text{O}$  content. The reaction temperature of this reactor was controlled by a water bath with a circulating pump, with an accuracy of  $\pm 0.1 \text{ }^\circ\text{C}$ . A FULI-9790 II gas chromatograph (GC; Fuli) was used to test the  $\text{H}_2\text{S}$ , COS and  $\text{CS}_2$  concentrations of the inlet and outlet gases.  $\text{H}_2\text{S}$ , COS and  $\text{CS}_2$  were tested by “Chromatographic column 1” (the peak appearance times of  $\text{H}_2\text{S}$ , COS and  $\text{CS}_2$  were 1.2 min, 1.5 min and 4.8 min, respectively). The conversion rate was calculated by the following equation.

$$\text{H}_2\text{S}(\text{COS}, \text{CS}_2) \text{ conversion } (\%) = \frac{\text{H}_2\text{S}(\text{COS}, \text{CS}_2)_{\text{inlet}} - \text{H}_2\text{S}(\text{COS}, \text{CS}_2)_{\text{outlet}}}{\text{H}_2\text{S}(\text{COS}, \text{CS}_2)_{\text{inlet}}} \times 100 \quad (1)$$

Sulfur capacity ( $\text{mgS/gcatalyst}$ ) is defined as the quality of sulfur deposition on the unit quality of WSBAC, with the conversion rate below 90%.

## Results and discussion

### Effect of carbonization temperature on simultaneous removal of $\text{H}_2\text{S}$ , COS and $\text{CS}_2$

The carbonization process could remove most of the organic composition and volatile components in the raw materials, which could increase the fixed carbon contents and reduce the ash content. This is the key step of producing WSBAC, because it could have the initial porosity with this step [19]. In this study, the influence of different carbonization temperatures (400, 500, 600, 700, 800  $^\circ\text{C}$ ) on the simultaneous removal of  $\text{H}_2\text{S}$ , COS and  $\text{CS}_2$  was investigated. In this section, other preparation conditions were: activator was KOH; activating agent content was 2:1 (mass ratio of KOH:WSBAC); activation temperature was 700  $^\circ\text{C}$ .

The desulfurization tests of WSBAC carbonized at different temperatures are shown in Fig. 2. From Fig. 2a, it can be seen that, with the increase of carbonization temperature, the maintaining time of 100%  $\text{CS}_2$  conversion firstly increased and then decreased. When the carbonization temperature was 400  $^\circ\text{C}$ , the 100% removal rate of  $\text{CS}_2$  could last for 360 min. When the carbonization temperature increased to 600  $^\circ\text{C}$ , the 100% removal rate of  $\text{CS}_2$  could last for 1140 min. However, the removal rate of  $\text{CS}_2$  was not increased with the increase of the carbonization temperature from 600 to 700  $^\circ\text{C}$ . When the carbonization temperature was increased to 700  $^\circ\text{C}$ , the 100% removal rate of  $\text{CS}_2$  lasted for 1080 min. From Fig. 2b, it can be seen that the removal efficiency trend of COS was similar to  $\text{CS}_2$ . The removal rate of COS was only 28% in the first 30 min when the carbonization temperature was 400  $^\circ\text{C}$ . When the carbonization temperature was increased to 600  $^\circ\text{C}$ , the first removal rate of COS achieved 100%, and the removal rate of COS was not increased with the increase of the carbonization temperature from 600 to 800  $^\circ\text{C}$ . From Fig. 2c, it can be seen that the removal efficiency trend of  $\text{H}_2\text{S}$  was also similar to  $\text{CS}_2$ . When the carbonization temperature was 400  $^\circ\text{C}$ , the 100% removal

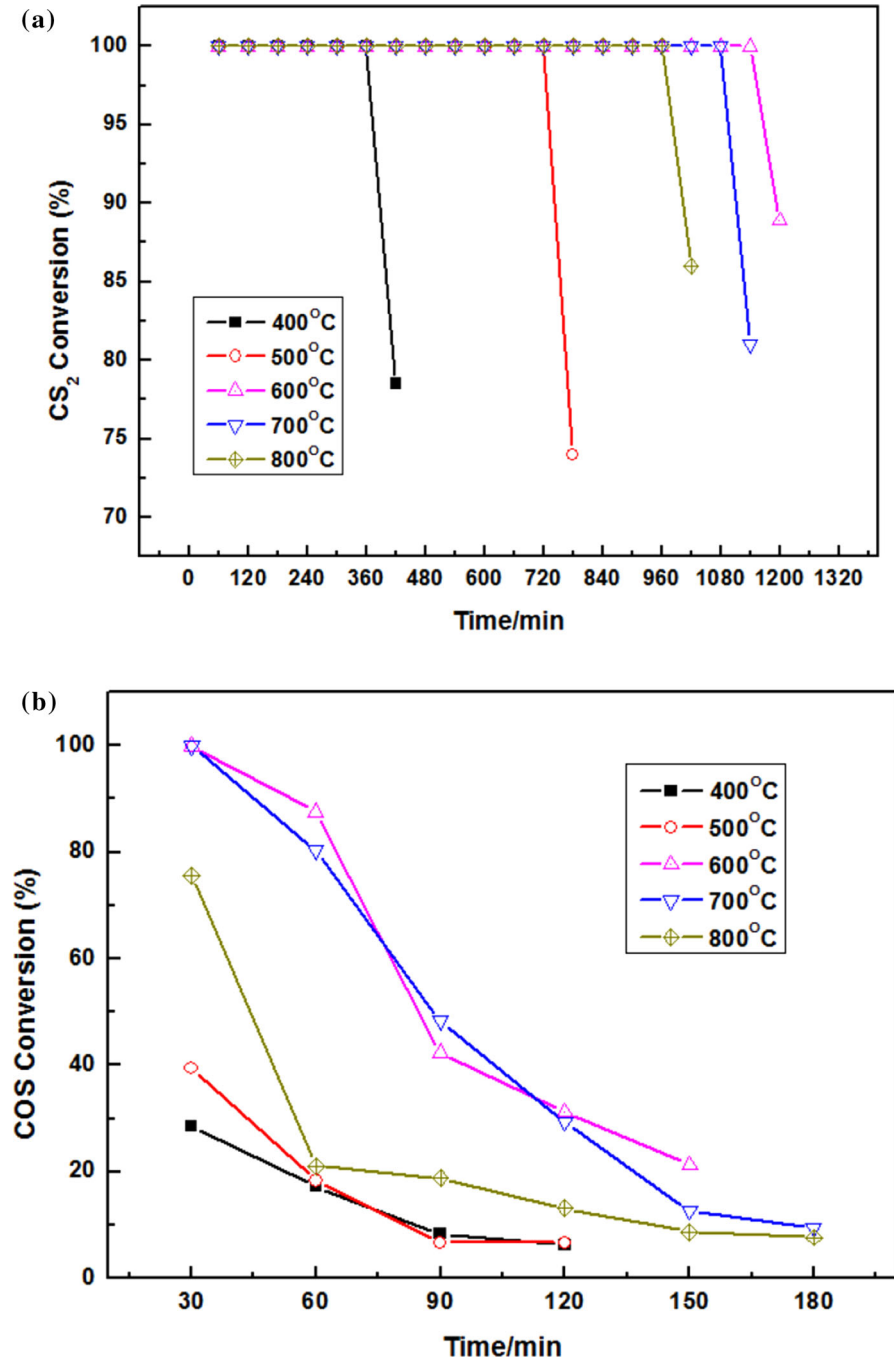


**Fig. 2** Effect of carbonization temperatures on the simultaneous removal of **a** CS<sub>2</sub>, **b** COS, **c** H<sub>2</sub>S, **d** sulfur capacity (reaction conditions: reaction temperature = 60 °C; RH = 49%; GHSV = 4000 h<sup>-1</sup>; H<sub>2</sub>S = 500 ppm; COS = 400 ppm; CS<sub>2</sub> = 50 ppm; O<sub>2</sub> = 0%)

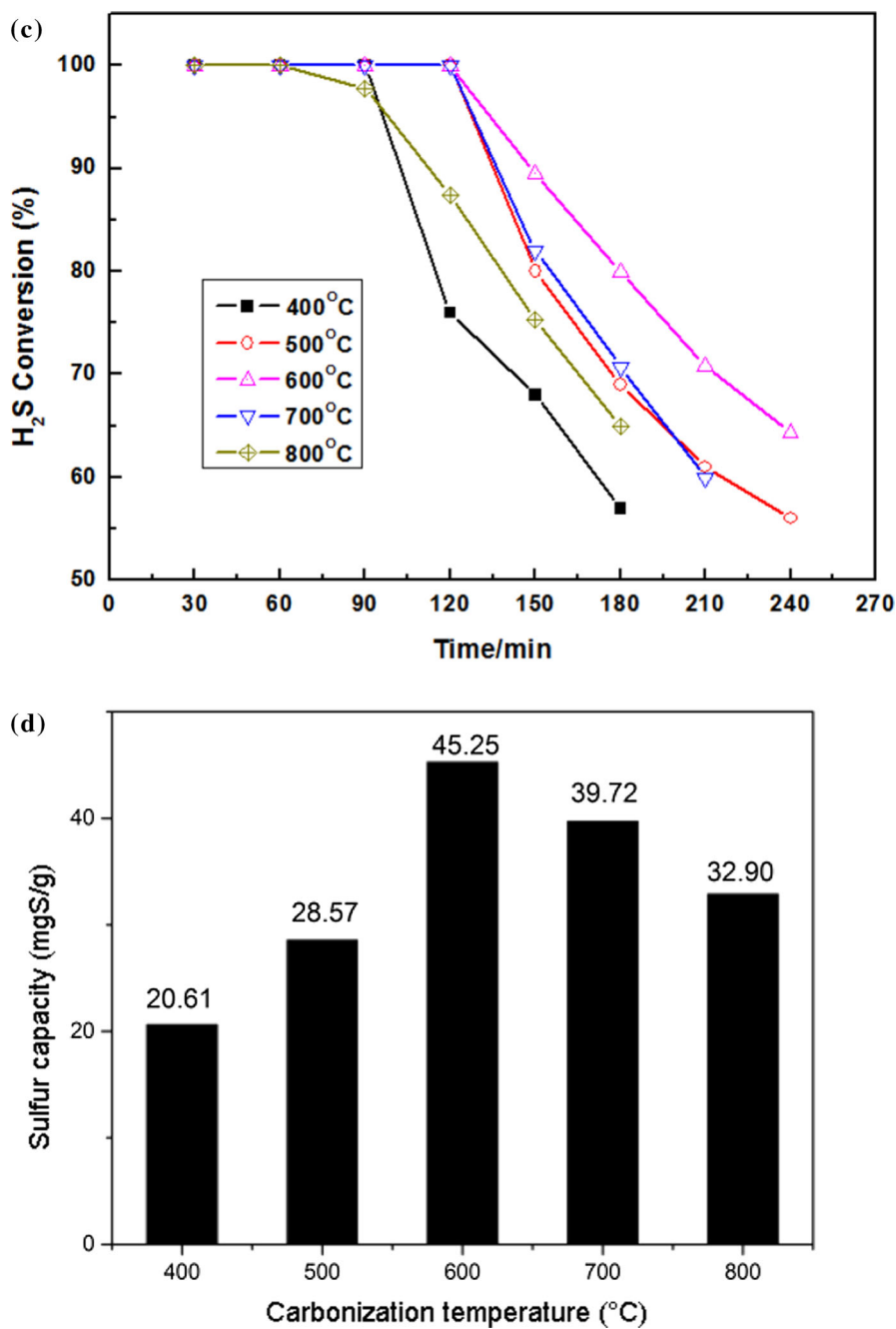


Fig. 2 continued

rate of H<sub>2</sub>S could last for 90 min. But the 100% removal rate of H<sub>2</sub>S could last for 120 min when the carbonization temperature was 600 °C.

Because of the optimum carbonization temperature for the removal of the three gases were not identical, the total sulfur capacity could be used to compare the removal ability of WSBAC with different carbonization temperatures. Figure 2d shows the sulfur content of WSBAC at different carbonization temperatures. With the increase of carbonization temperature, the sulfur content of WSBAC first increased and then decreased. When the carbonization temperature was 600 °C, the WSBAC had the highest sulfur content (45.25 mgS/g<sub>WSBAC</sub>).

The carbonization process could mainly produce initial porosity and pore size, and the number determines the pore volume. This is one of the main factors influencing the removal performances of WSBAC. At the lower carbonization temperature, fewer initial pores were produced in the raw material. With the increase of temperature, the initial hole increases. When the temperature is lower, the initial pore may be mainly mesoporous, and with the increase of carbonization temperature, the micropores start to appear. When the carbonization temperature is too high, micropores can collapse and the polycondensation reaction results in microporous decreasing dramatically and mesoporous increasing a great deal [20]. However, micropores can play a major role in the gas adsorption, the number and volume of the micropores determining the WSBAC specific surface area, surface adsorption sites and adsorption capacity. This is an important factor that affects the simultaneous removal ability of H<sub>2</sub>S, COS and CS<sub>2</sub> over WSBAC.

To investigate the influence of carbonization temperature on pore structure and surface area, BET analyses were carried out and are shown in Fig. 3 and Table 1. From the BET results (Table 1), can be seen that the sample had the highest surface area and most micropores when the carbonization temperature was 600 °C, which enhanced the adsorptive capacity of the WSBAC. This result indicated that the increase of carbonization temperature could increase the surface area, which was attributed to the increase of micropores and decrease of mesoporous. When the carbonization temperature was 500 °C, the walnut shells had not been completely carbonized [21], and they had low surface area and micropore volume. When the carbonization temperature rose to 600 °C, the surface area and micropore volume increased from 678.30 to 1239.92 m<sup>2</sup>/g and 0.367 to 0.673 cm<sup>3</sup>/g, respectively. This indicated that the suitable carbonization temperature was conducive to the generation of micropores. When the carbonization temperature rose to 700 °C, the surface area and micropore volume decreased. This was attributed to the conversion of micropores to mesopores [22]. As a result, the specific surface area decreased, and the removal efficiencies of H<sub>2</sub>S, COS and CS<sub>2</sub> were decreased.

Figure 3a shows the nitrogen adsorption isotherms of three samples with different carbonization temperatures (500, 600, 700 °C). According to the IUPAC classification, the adsorption isotherms of the three samples are of type I which indicates that they are predominantly microporous materials. Meanwhile, the N<sub>2</sub> accumulation adsorbing capacity of WSBAC with carbonization temperature of 600 °C is higher than that of the other two samples with carbonization temperatures of 500 and 700 °C. Furthermore, Fig. 3b shows that micropores were mainly at 0.3–1.8 nm. From Fig. 3b, it can be observed that, when the carbonization

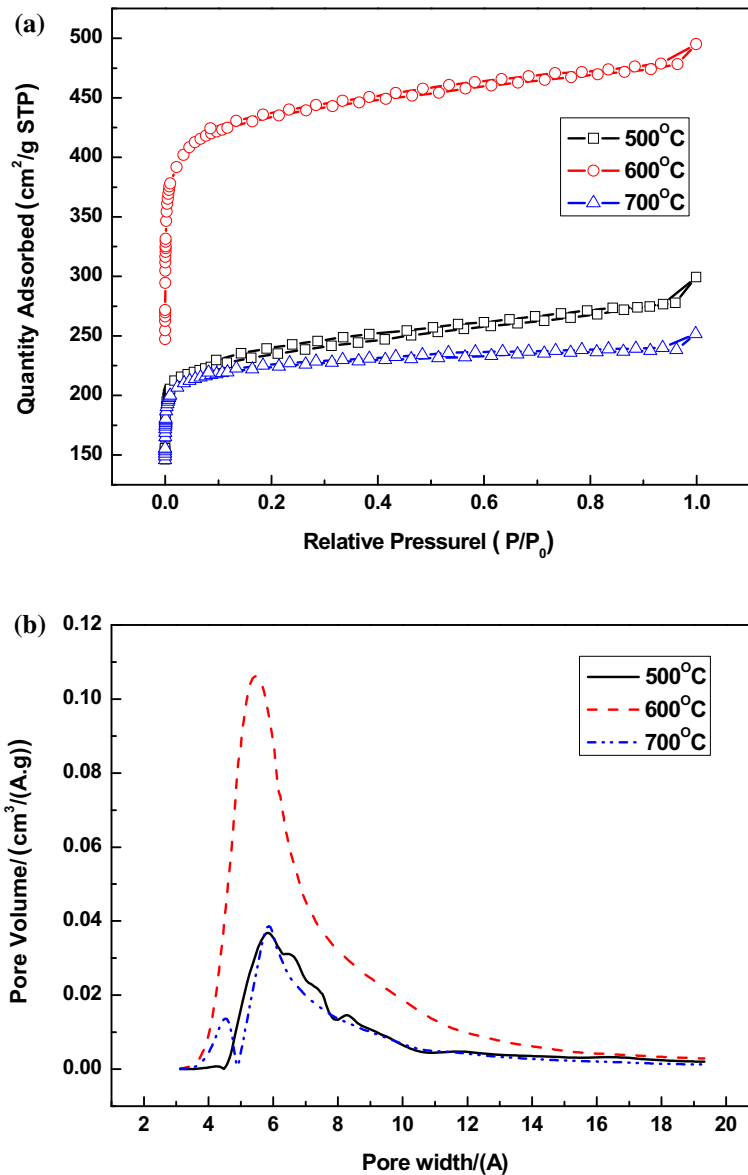


**Fig. 3** a Nitrogen adsorption isotherms for three samples carbonized at different temperatures. b Pore size distribution (< 20 Å) for three samples carbonized at different temperatures

temperature was 600 °C, the WSBAC sample had higher micropore volume, at 0.3–1.8 nm, than those of the other two samples. This indicates that micropores at 0.3–1.8 nm play an important role for the simultaneous removal of H<sub>2</sub>S, COS and CS<sub>2</sub>.



**Table 1** Porosity parameters of WSBAC carbonized at different temperatures

Activation temperature (°C)	Surface area (m <sup>2</sup> g <sup>-1</sup> )	Total pore volume (cm <sup>3</sup> g <sup>-1</sup> )	Micropore volume (cm <sup>3</sup> g <sup>-1</sup> )	Mesoporous volume (cm <sup>3</sup> g <sup>-1</sup> )
500	678.30	0.463	0.367	0.096
600	1239.92	0.766	0.673	0.093
700	634.12	0.246	0.205	0.041

### Effect of activating agent species on simultaneous removal of H<sub>2</sub>S, COS and CS<sub>2</sub>

The activation process of the walnut shells can further produce a large number of pores, so as to increase pore number, higher pore volume and specific surface area [23]. This is also an important step to prepare the WSBAC. In this study, four kinds of common activators (ZnCl<sub>2</sub>, KOH, H<sub>3</sub>PO<sub>4</sub>, K<sub>2</sub>CO<sub>3</sub>) were selected to activate the carbonized materials, and the influence of the type of activator on the simultaneous removal of H<sub>2</sub>S, COS and CS<sub>2</sub> was studied. In this section, other preparation conditions were: carbonization temperature was 600 °C; activating agent content was 2:1 (mass ratio of activating agent:WSBAC); activation temperature was 700 °C. The desulfurization tests of WSBAC activated with different activators are shown in Fig. 4, from which it can be seen that KOH is the best activator for simultaneously removing H<sub>2</sub>S, COS and CS<sub>2</sub>. The activity order of four activators is KOH > K<sub>2</sub>CO<sub>3</sub> > H<sub>3</sub>PO<sub>4</sub> > ZnCl<sub>2</sub>. For the sample that KOH activated, the 100% removal rate of CS<sub>2</sub> could last for 1200 min, the 100% removal rate of COS could last for 30 min, and 100% removal rate of H<sub>2</sub>S could last for 120 min.

According to Fig. 4d, it is clear that the sulfur capacities of WSBAC activated with KOH and K<sub>2</sub>CO<sub>3</sub> are higher than that of ZnCl<sub>2</sub> and H<sub>3</sub>PO<sub>4</sub>. The sulfur capacity of WSBAC activated with KOH is 45.25 mgS/g<sub>WSBAC</sub>, but the sulfur capacity of WSBAC activated with H<sub>3</sub>PO<sub>4</sub> is only 2.5 mgS/g<sub>WSBAC</sub>. Because the KOH can react with the carbon material under high-temperature conditions, it can make a large number of micropores inside the carbon material [24].

WSBAC activated by KOH and K<sub>2</sub>CO<sub>3</sub> also showed higher desulfurization efficiency, and generated molten metal K because of the high temperature, which could reduce the surface tension of the carbon [25, 26]. There is only a very low sulfur capacity of WSBAC activated by H<sub>3</sub>PO<sub>4</sub> and ZnCl<sub>2</sub>. As activator, the KOH could not only provide K<sup>+</sup> in the process of activation but also offer a lot of OH<sup>-</sup> and ·OH functional groups in the process of activation [27]. OH<sup>-</sup> increased the WSBAC to adsorb sulfur gas, and ·OH also strengthened the alkaline adsorption sites of the WSBAC. Furthermore, the content of the surface functional groups was affected by the pore structure and surface area. To investigate the influence of the activator on the pore structure and surface area, BET analyses were carried out and are shown in Fig. 5 and Table 2.

From the BET results (Table 2), it is shown that the WSBAC sample had the highest surface area (1239.92 m<sup>2</sup>/g) and most micropore volume (0.673 cm<sup>3</sup>/g) when it was activated by KOH. ZnCl<sub>2</sub> and H<sub>3</sub>PO<sub>4</sub> offered little micropore volume

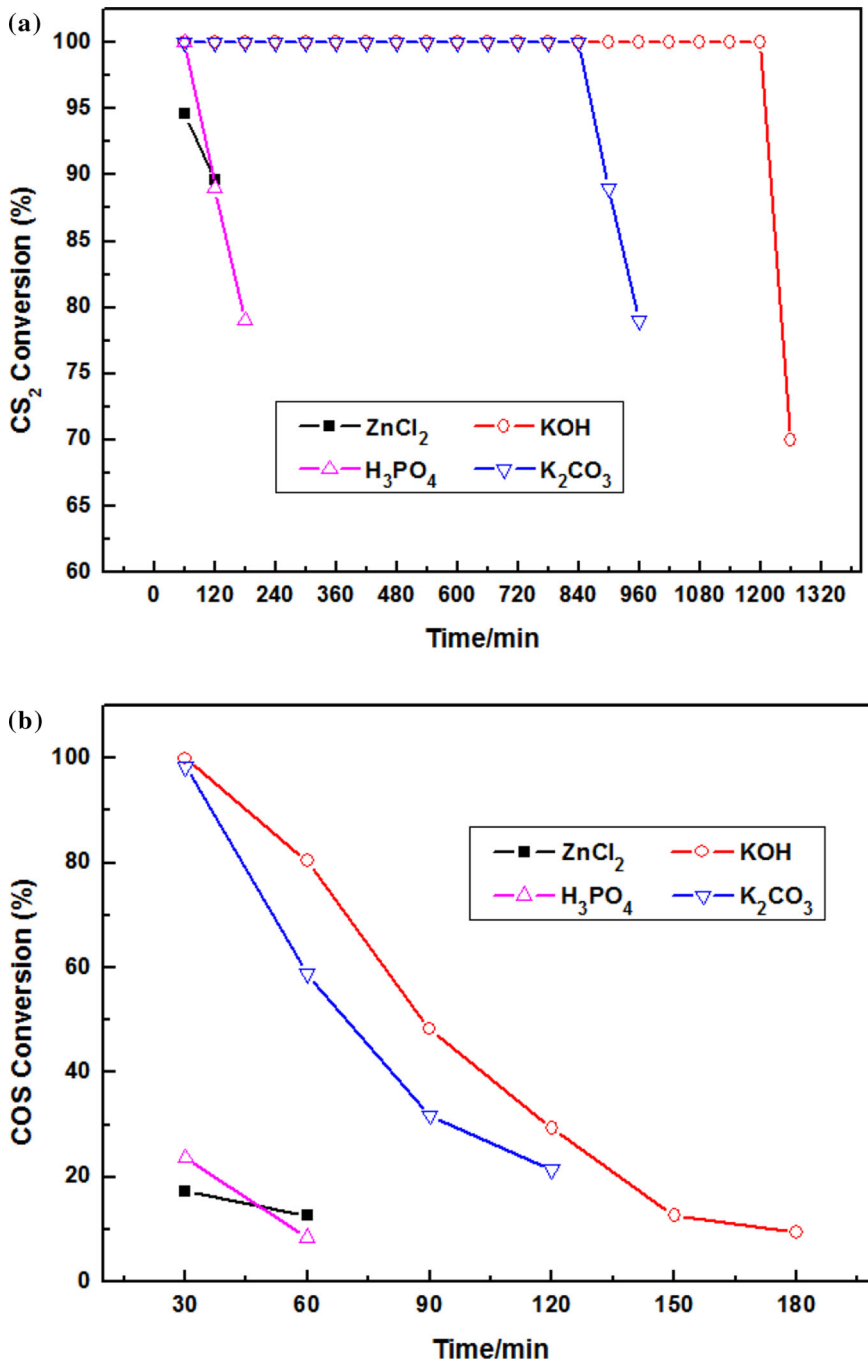


**Fig. 4** Effect of activating agent species on removal of **a** CS<sub>2</sub>, **b** COS, **c** H<sub>2</sub>S, **d** sulfur capacity (reaction conditions: reaction temperature = 60 °C; RH = 49%; GHSV = 4000 h<sup>-1</sup>; CS<sub>2</sub> = 50 ppm; COS = 400; H<sub>2</sub>S = 500 ppm; O<sub>2</sub> = 0%)

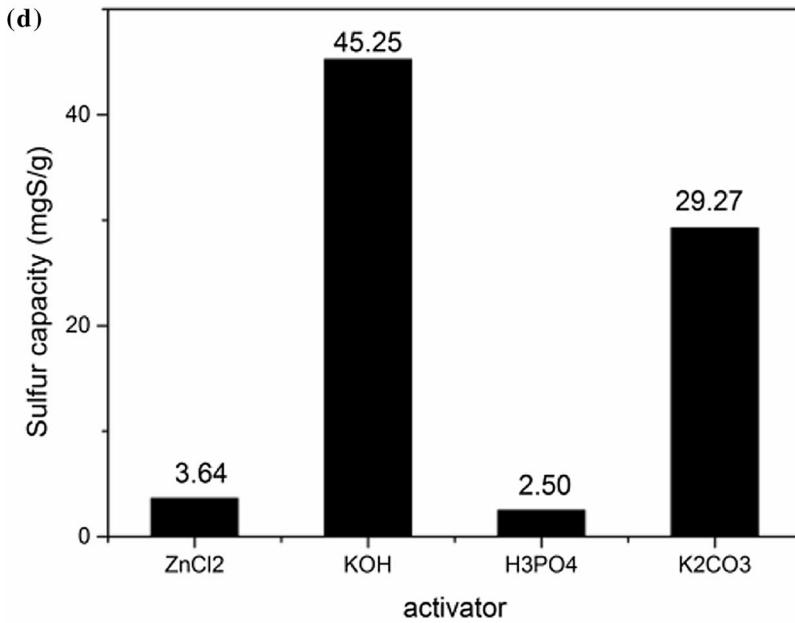
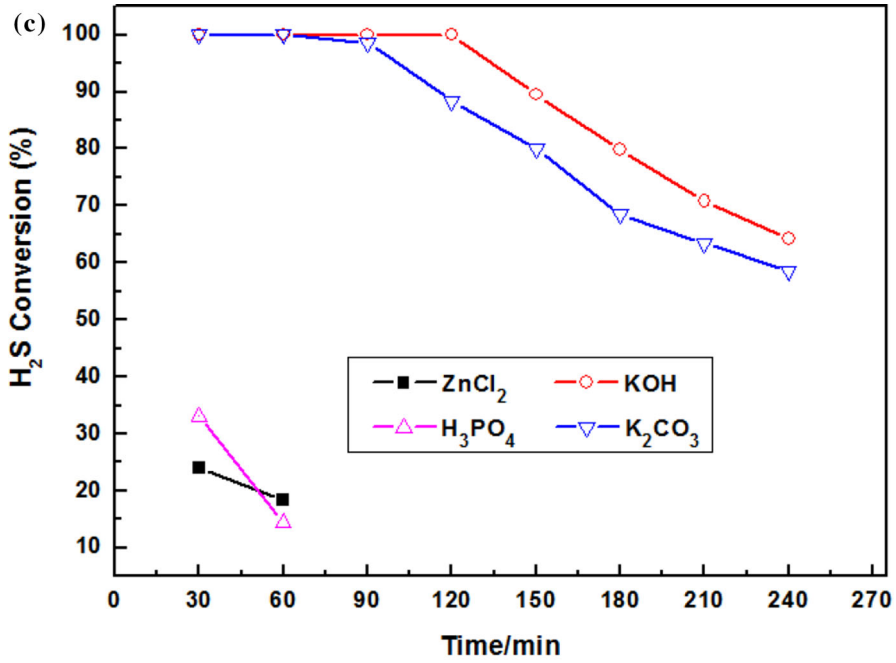
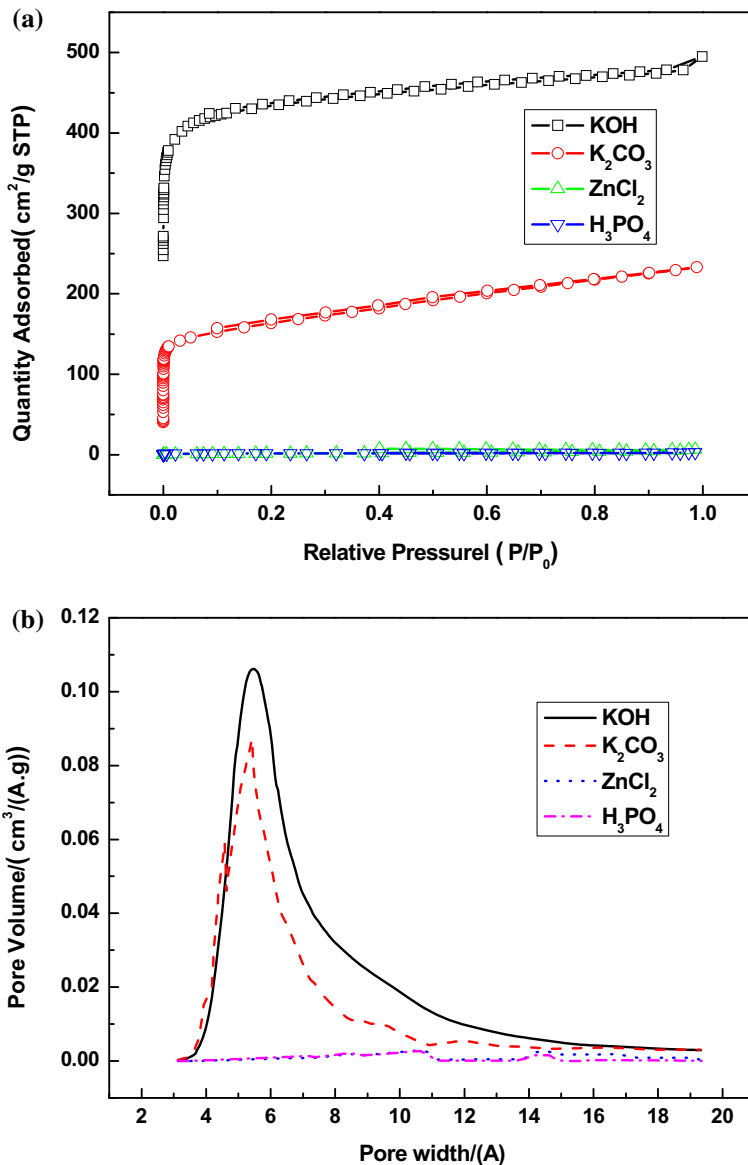


Fig. 4 continued



**Fig. 5** **a** Nitrogen adsorption isotherms of WSBAC activated with different activators. **b** Pore size distribution (< 20 Å) for WSBAC activated with different activators

and surface area, which was not conducive to the adsorptive capacity of WSBAC. Figure 5a shows the nitrogen adsorption isotherms of WSBAC activated by different activators (KOH,  $K_2CO_3$ ,  $ZnCl_2$  and  $H_3PO_4$ ). According to the IUPAC classification, the adsorption isotherms of two samples (KOH,  $K_2CO_3$ ) are of type I, which indicates that they are predominantly microporous materials. Meanwhile, the

**Table 2** Porosity parameters of WSBAC activated with different activators

Activator	Surface area ( $\text{m}^2 \text{g}^{-1}$ )	Total pore volume ( $\text{cm}^3 \text{g}^{-1}$ )	Micropore volume ( $\text{cm}^3 \text{g}^{-1}$ )	Mesoporous volume ( $\text{cm}^3 \text{g}^{-1}$ )
KOH	1239.92	0.766	0.673	0.093
$\text{K}_2\text{CO}_3$	607.18	0.340	0.245	0.095
$\text{ZnCl}_2$	5.95	0.011	0.006	0.005
$\text{H}_3\text{PO}_4$	1.28	0.005	0.002	0.003

$\text{N}_2$  accumulation adsorbing capacity of WSBAC activated by KOH is higher than that of other three WSBAC which indicates that KOH was conducive to generate more micropores. From Fig. 5b, it can be observed that the WSBAC activated by KOH has higher pore volume, at 0.3–1.8 nm, than those of the other three WSBAC, which indicates that KOH could generate more micropores at 0.3–1.8 nm. Therefore, KOH is the optimized activator.

### Effect of activating agent content on simultaneous removal of $\text{H}_2\text{S}$ , COS and $\text{CS}_2$

The activating agent content is a main influencing factor for micropore volume, micropore quantity, and micropore superficial area. In this study, the effect of different activating agent contents on the simultaneous removal of  $\text{CS}_2$ , COS and  $\text{H}_2\text{S}$  was studied. In this section, other preparation conditions were: carbonization temperature was 600 °C; activator was KOH; activation temperature was 700 °C.

The desulfurization tests of WSBAC activated at different temperatures are shown in Fig. 6. From Fig. 6a, it can be seen that, with the increase of activator content, the  $\text{CS}_2$  removal rate was firstly increased and then subsequently decreased. When the activating agent content was 0.25, the 100% removal rate of  $\text{CS}_2$  could last for 720 min. When the activating agent content increased to 1, the 100% removal rate of  $\text{CS}_2$  could last for 1440 min. But the removal rate of  $\text{CS}_2$  was not increased with the increase of the activating agent content. When the activating agent content was 2, the 100% removal rate of  $\text{CS}_2$  could last for 1140 min. From Fig. 6b, it can be seen that, with the increase of activating agent content, the removal of COS firstly increased and then decreased. When the activating agent content was 0.25, the removal rate of COS was only 52%, and the removal rate of COS decreased as the reaction progressed. When the activating agent content increased to 1, the first removal rate of COS was 100%, and the removal rate of COS decreased as the reaction progressed. But the removal rate of COS was not increased with the increase of the activating agent content. When the activating agent content was 1.5, the removal rate of COS was only 79%. From Fig. 6c, it can be seen that, with the increase of activating agent content, the removal of  $\text{H}_2\text{S}$  firstly increased and then decreased. When the activating agent content was 0.25, the removal rate of  $\text{H}_2\text{S}$  was only 53%, and the removal rate of  $\text{H}_2\text{S}$  decreased as the reaction progressed. When the activating agent content increased to 0.5, the 100% removal

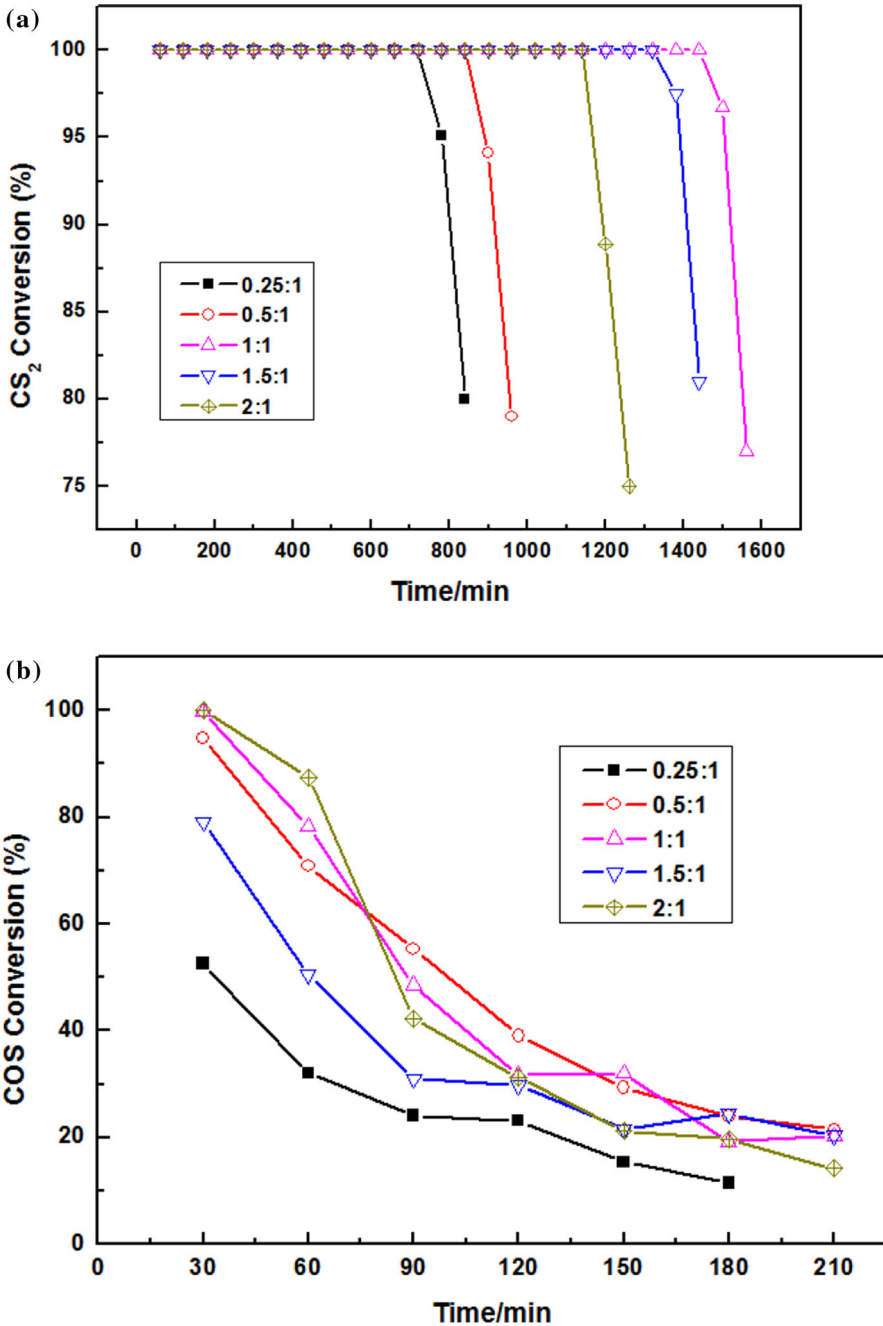


**Fig. 6** Effect of activating agent content on removal of **a** CS<sub>2</sub>, **b** COS, **c** H<sub>2</sub>S, **d** sulfur capacity (reaction conditions: reaction temperature = 60 °C; RH = 49%; GHSV = 4000 h<sup>-1</sup>; CS<sub>2</sub> = 50 ppm; COS = 400 ppm; H<sub>2</sub>S = 500 ppm; O<sub>2</sub> = 0%)

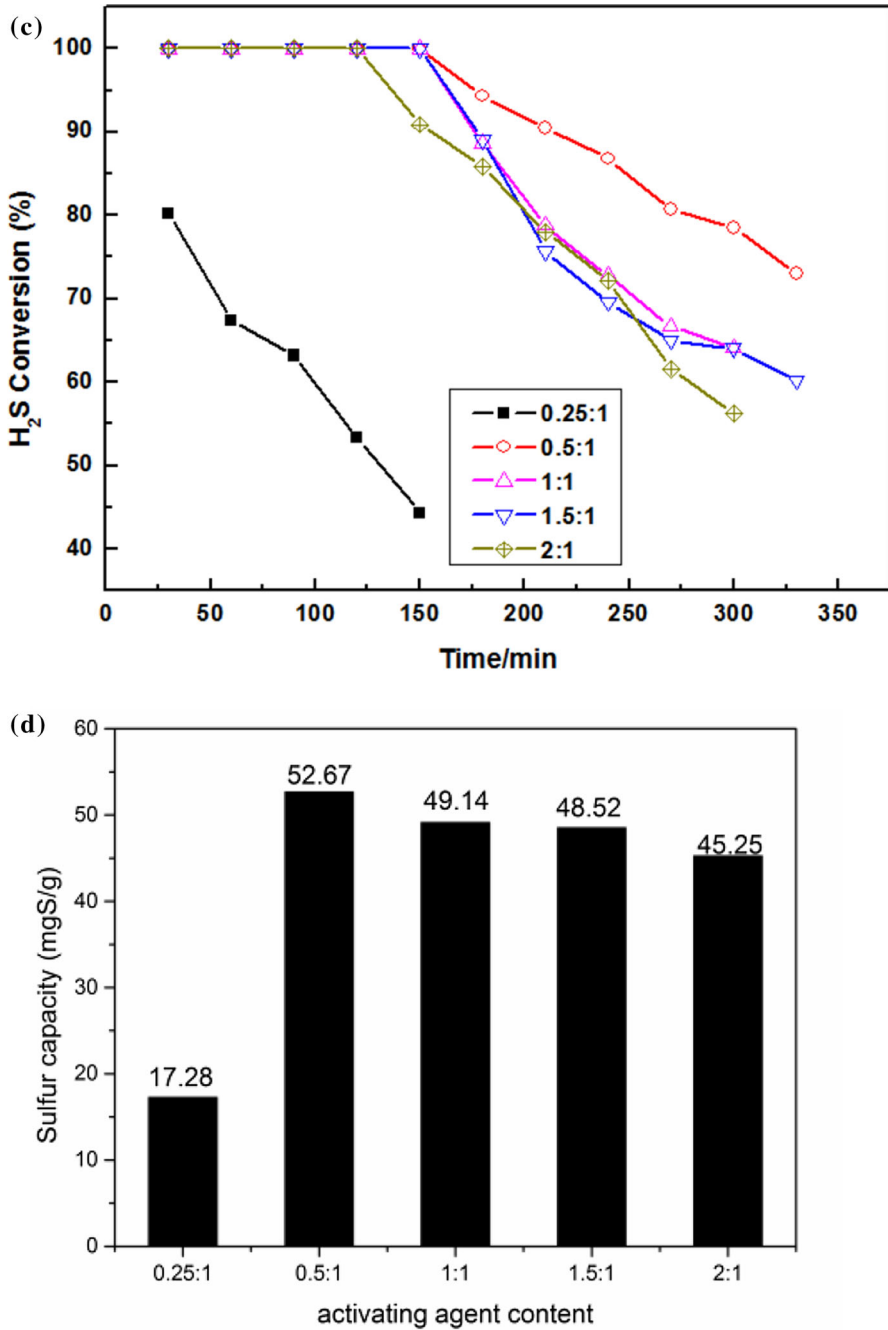


Fig. 6 continued

rate of  $\text{H}_2\text{S}$  could last for 150 min. But the 100% removal rate of  $\text{H}_2\text{S}$  could last for 120 min, when the activating agent content increased to 2.

Figure 6d shows the sulfur content of WSBAC for different activating agent contents. With the increase of the activating agent content, the sulfur content of WSBAC increased and then decreased. When the activating agent content was 0.5, the activated carbon of WSBAC had the highest sulfur content. The highest sulfur content is  $52.67 \text{ mgS/g}_{\text{WSBAC}}$ .

Activator content mainly affects the efficiency of the activation and generation of pore volume. Under the lower activator content, the raw materials are not fully activated, few micropores can be produced inside the WSBAC, and the surface area and the number of adsorption sites may be fewer. With the increase of content of the activator, the activation reaction becomes fuller, and the microporous will be increased. However, when the activator amount was excessive, the adsorption performance of WSBAC did not continue to increase. Because the excessive activator could block the micropore structure, the quantity and volume of pores, the specific surface area and surface adsorption sites of WSBAC would be reduced, which leads to the decrease of the adsorption capacity of WSBAC. To investigate the influence of activating agent content on the pore structure and surface area, BET analyses were carried out and are shown in Fig. 7 and Table 3.

With the decreasing of KOH contents from 2 to 0.5 times, the sulfur content of the WSBAC had a minor improvement. So the two samples (0.5 and 2 times of KOH) were tested by BET. The BET results (Table 3) show that the sample had the highest surface area ( $1239.92 \text{ m}^2/\text{g}$ ) and most micropore volume ( $0.673 \text{ cm}^3/\text{g}$ ) when the activating agent content was 2. Figure 7a shows the nitrogen adsorption isotherms of the two samples. According to the IUPAC classification, the adsorption isotherms of two samples are type I which indicates that they are predominantly microporous materials. Although the  $\text{N}_2$  accumulation adsorbing capacity of WSBAC activated by 2 times of KOH was higher than that of the other one, the WSBAC activated by 0.5 times of KOH had a higher sulfur content which might be affected by the micropore width. From Fig. 7b, it can be seen that WSBAC activated by 0.5 times of KOH has a higher micropore volume, at 0.3–0.5 nm, than that of WSBAC activated by 2 times of KOH. This indicates that the micropore at 0.3–0.5 nm played a more important role in the simultaneous removal of  $\text{H}_2\text{S}$ , COS and  $\text{CS}_2$ . Meanwhile, the high activating agent content led to an excessive activation, which could widen the pore width [28].

### **Effect of activation temperature on simultaneous removal of $\text{H}_2\text{S}$ , COS and $\text{CS}_2$**

Activation temperature can influence the WSBAC's activation process, especially for the pore structure. Therefore, it is important to investigate this influence. In this study, the effect of activation temperatures (600, 700, 800, 900 °C) on removal of  $\text{H}_2\text{S}$ , COS and  $\text{CS}_2$  has been studied. In this section, other preparation conditions were: carbonization temperature was 600 °C; activator was KOH; activating agent content was 0.5:1 (mass ratio of KOH:WSBAC).



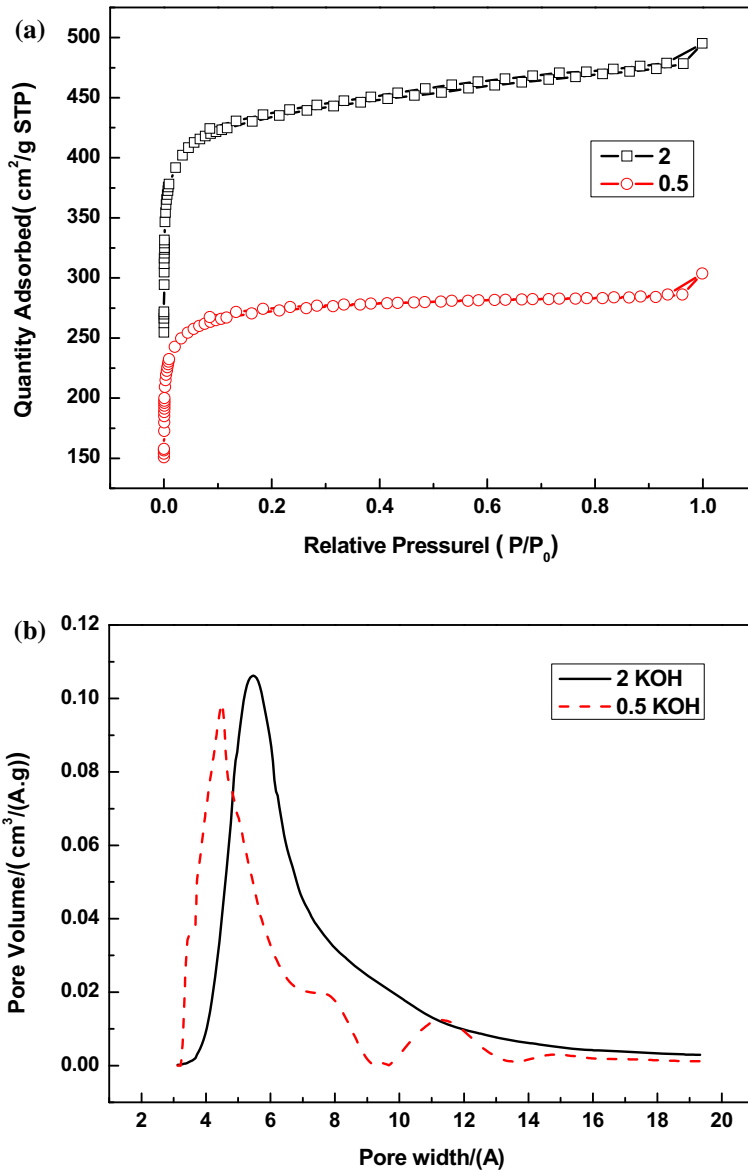


**Fig. 7** a Nitrogen adsorption isotherms for WSBAC activated with different of activating agent contents. b Pore size distribution (< 20 Å) for WSBAC activated with different of activating agent contents

The desulfurization tests of WSBAC activated at different temperatures are shown in Fig. 8. From Fig. 8a, it can be seen that, with the increase of activation temperature, the removal of CS<sub>2</sub> firstly increased and then decreased. When the activation temperature was 600 °C, the removal rate of 100% CS<sub>2</sub> could last for 360 min. When the activation temperature increased to 700 °C, the removal rate of

**Table 3** Porosity parameters of WSBAC activated with different of activating agent contents

Activating agent content	Surface area ( $\text{m}^2 \text{g}^{-1}$ )	Total pore volume ( $\text{cm}^3 \text{g}^{-1}$ )	Micropore volume ( $\text{cm}^3 \text{g}^{-1}$ )	Mesoporous volume ( $\text{cm}^3 \text{g}^{-1}$ )
2	1239.92	0.766	0.673	0.093
0.5	484.26	0.272	0.261	0.011

100%  $\text{CS}_2$  could last for 840 min. However, the removal rate of  $\text{CS}_2$  was not increased with the increase of the carbonization temperature from 700 to 800 °C. When the activation temperature was 800 °C, the 100% removal rate of  $\text{CS}_2$  lasted for 720 min. From Fig. 8b, it can be seen that, with the increase of activation temperature, the removal of COS firstly increased and then decreased. When the activation temperature was 600 °C, the removal rate of COS was only 42% in the first 30 min. When the activation temperature was increased to 700 °C, the first removal rate of COS was 100%. However, the removal rate of COS was not increased with the increase of the activation temperature from 700 to 800 °C. From Fig. 8c, it can be seen that, with the increase of activation temperature, the removal of  $\text{H}_2\text{S}$  firstly increased and then decreased. When the activation temperature was 600 °C, the removal rate of  $\text{H}_2\text{S}$  was only 85% in the first 30 min. When the activation temperature was increased to 700 °C, the 100% removal rate of  $\text{H}_2\text{S}$  could last for 150 min. However, the removal rate of  $\text{H}_2\text{S}$  was not increased with the increase of the activation temperature. When the activation temperature was increased to 900 °C, the 100% removal rate of  $\text{H}_2\text{S}$  could last for 30 min.

Figure 8d shows the sulfur content of WSBAC at different activation temperatures. With the increase of the activation temperature, the sulfur content of WSBAC first increased and then decreased. When activation temperature was 700 °C, the WSBAC has the highest sulfur content, which is 52.67  $\text{mgS/g}_{\text{WSBAC}}$ .

Activation temperature can affect the KOH activation mechanism, thus affecting the WSBAC's pore structure and specific surface. When the activation temperature is low, the activator can only occur on the dehydration of itself and the reaction with the functional groups on the surface of the carbon materials. As the activation process cannot get enough energy, the activation efficiency is low, so that the micropore structure is not developed. With the increase of the activation temperature, the activation process can obtain enough energy and large numbers of microporous can be produced at this stage. However, when the activation temperature is too high, the activity of the activator is extreme and this shows that extreme activation of  $\text{K}^+$  shuttles back and forth on the carbon, and will not only produce more micropore but also expand micropores to mesopores or macropores. Thus, the number of pores and the volume of the micropores can be decreased, leading to reduced adsorption performance. To investigate the influence of activation temperature on the pore structure and surface area, BET analyses were carried out and are shown in Fig. 9 and Table 4.

From Table 4, when the activation temperature increased from 600 to 700 °C, the surface area and the micropore volume increased from 125.97 to 484.26  $\text{m}^2/\text{g}$  and 0.066 to 0.261  $\text{cm}^3/\text{g}$ , respectively, which indicated that a suitable activation

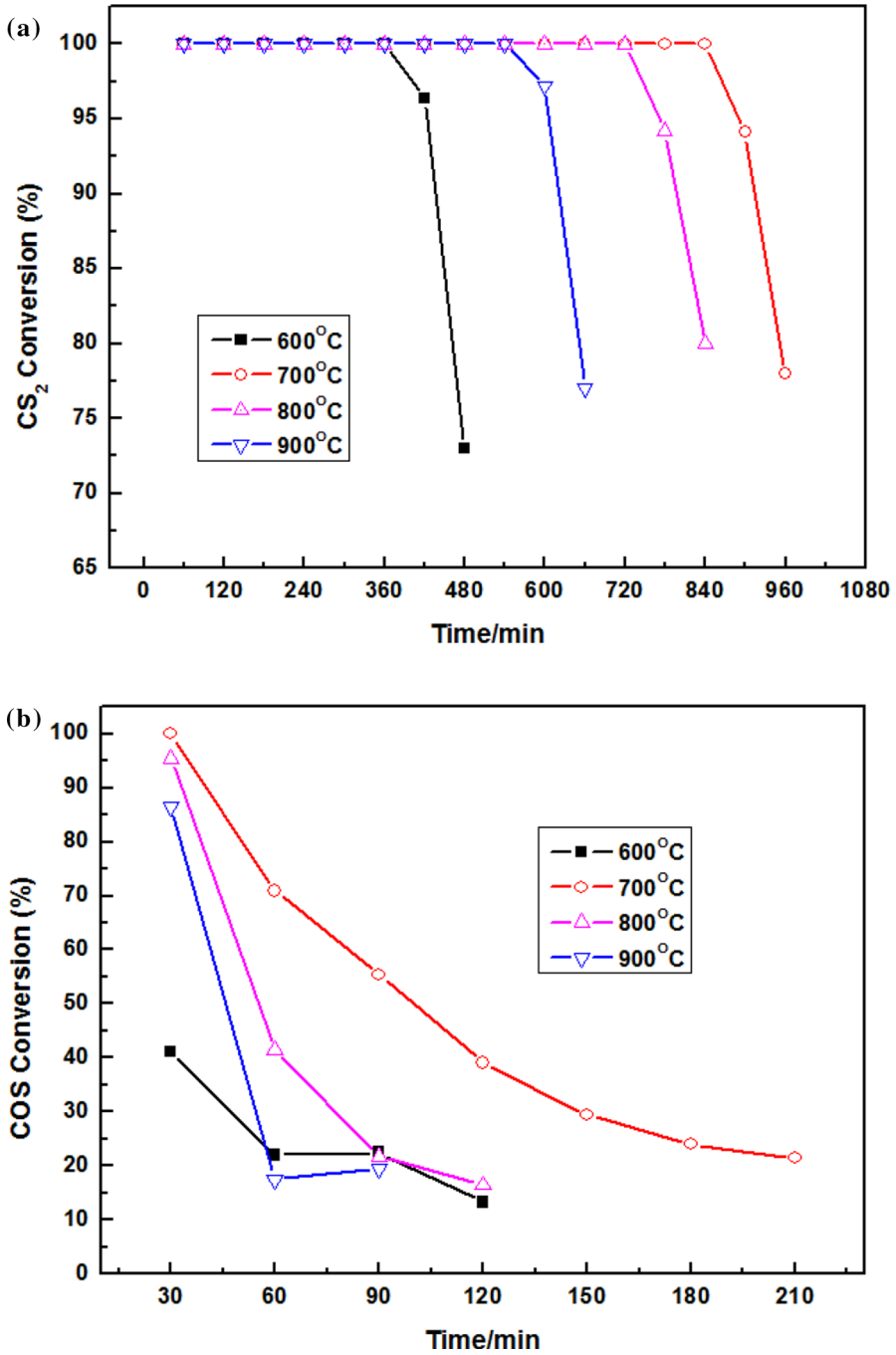


**Fig. 8** Effect of activation temperature on removal of **a** CS<sub>2</sub>, **b** COS, **c** H<sub>2</sub>S, **d** sulfur capacity (reaction conditions: reaction temperature = 60 °C; RH = 49%; GHSV = 4000 h<sup>-1</sup>; CS<sub>2</sub> = 50 ppm; COS = 400 ppm; H<sub>2</sub>S = 500 ppm; O<sub>2</sub> = 0%)

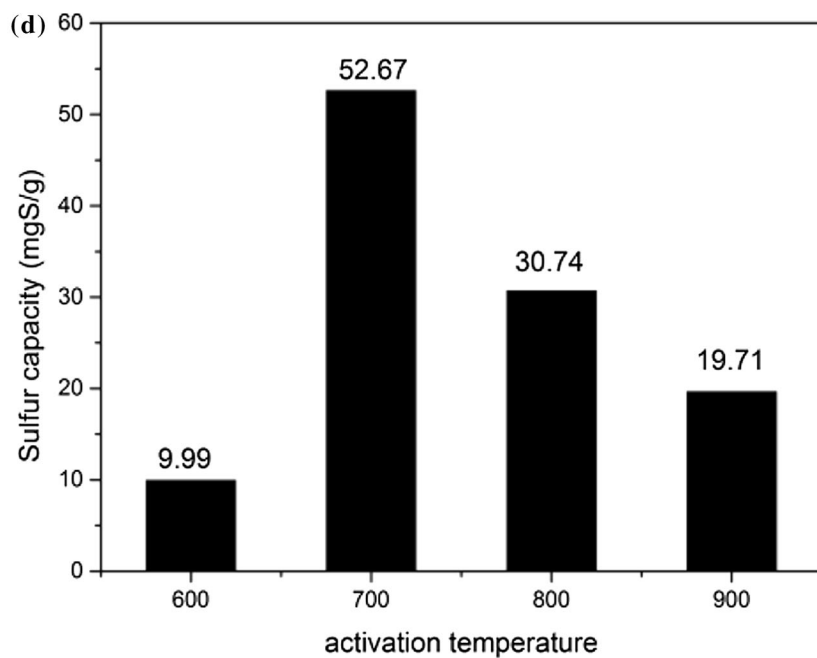
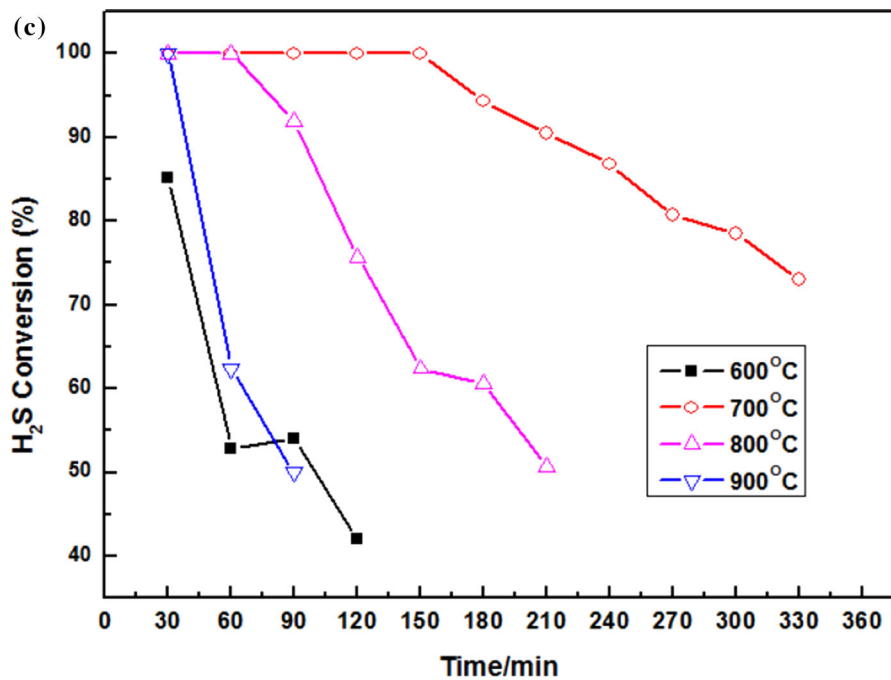
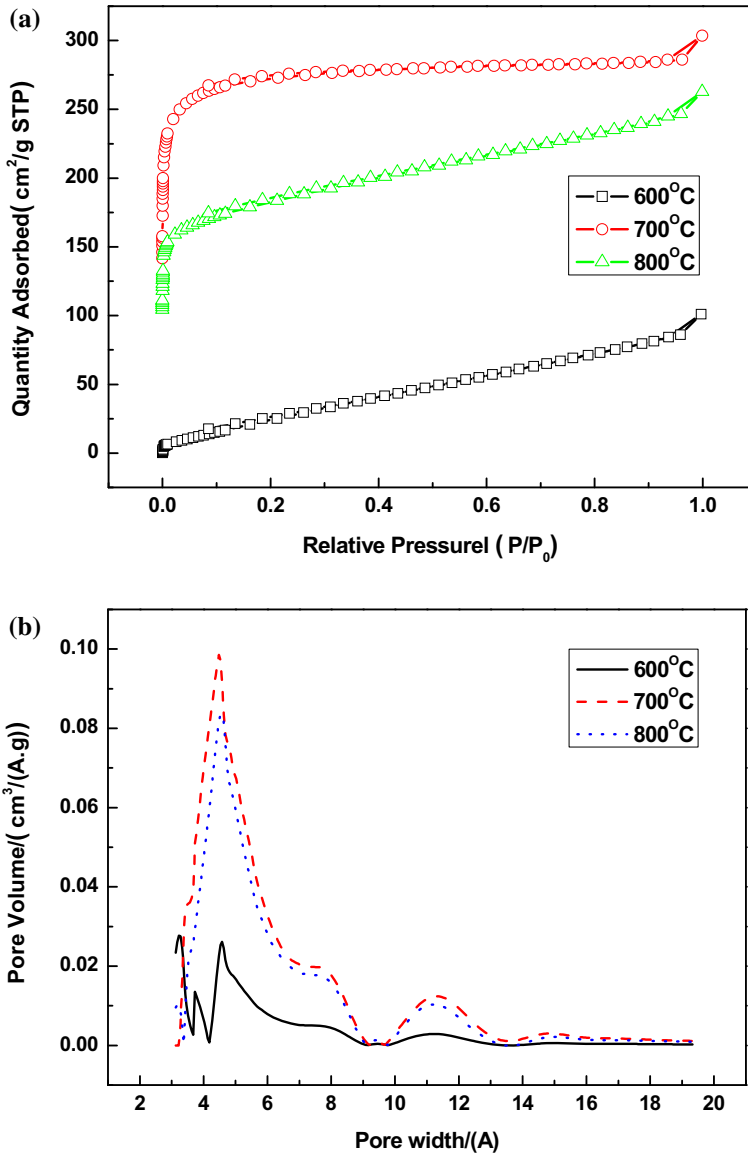


Fig. 8 continued

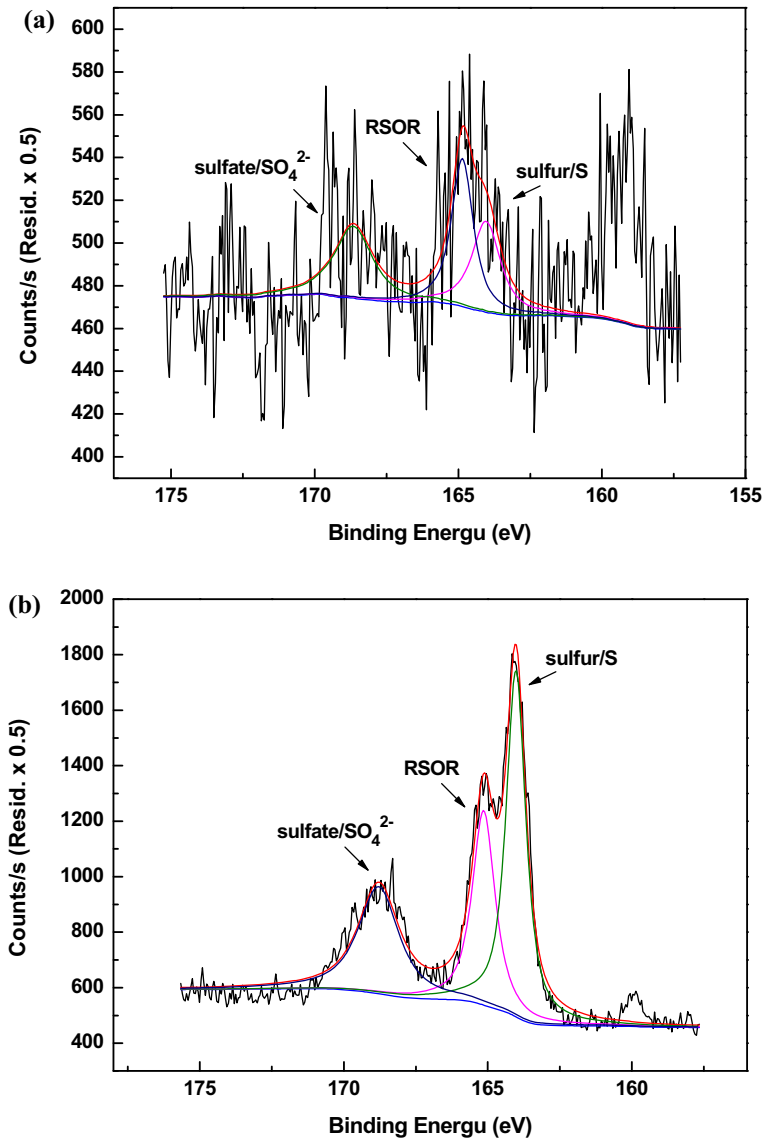


**Fig. 9** **a** Nitrogen adsorption isotherms for WSBAC activated at different temperatures. **b** Pore size distribution ( $< 20 \text{ \AA}$ ) for WSBAC activated at different temperatures

temperature was conducive to the generation of a micropore structure. When the activation temperature rose to 800 °C, the surface area and the micropore area of the WSBAC decreased slightly from 484.26 to 447.58 m<sup>2</sup>/g and 0.261 to 0.236 cm<sup>3</sup>/g, respectively, which indicated that an excessively high activation temperature converted the micropores to mesoporous [29], which led to the removal efficiency of CS<sub>2</sub>, COS and H<sub>2</sub>S being decreased.

**Table 4** Porosity parameters of WSBAC activated at different temperatures

Activation temperature (°C)	Surface area (m <sup>2</sup> g <sup>-1</sup> )	Total pore volume (cm <sup>3</sup> g <sup>-1</sup> )	Micropore volume (cm <sup>3</sup> g <sup>-1</sup> )	Mesoporous volume (cm <sup>3</sup> g <sup>-1</sup> )
600	125.97	0.072	0.066	0.006
700	484.26	0.272	0.261	0.011
800	447.58	0.255	0.236	0.019

**Fig. 10** Detail S2p XPS spectra of **a** fresh WSBAC, **b** exhausted WSBAC

**Table 5** Surface S2p elemental analysis of fresh and exhausted WSBAC

Element	Fresh WSBAC (at.%)	Exhausted WSBAC (at.%)
S2p	0.135	1.49

**Table 6** Surface content of S species on fresh and exhausted WSBAC

WSBAC	S2p (at.%)		
	164.0 eV	165.1 eV	168.8
Fresh sample	0.041	0.052	0.042
Inactivation sample	0.652	0.422	0.415

Figure 9a shows the nitrogen adsorption isotherms of three samples with different activation temperatures (600, 700, 800 °C). According to the IUPAC classification, the adsorption isotherms of the three samples are of type I, which indicates that they are predominantly microporous materials. Meanwhile, when the activation temperature was 700 °C, the N<sub>2</sub> accumulation adsorbing capacity of WSBAC was higher than those of the other two samples. Furthermore, from Fig. 9b, it can be observed that the WSBAC activated at 700 °C has a higher micropore volume, at 0.3–1.8 nm, than those of the other two. This indicates that the micropores at 0.3–1.8 nm played a more important role for the simultaneous removal of H<sub>2</sub>S, COS and CS<sub>2</sub>. Therefore, 700 °C is the most suitable activation temperature.

The pore structure and surface characteristics were also affected by surface species in the reaction, especially for the deactivation process. Therefore, it is important to investigate the change of surface species. To do so, XPS analyses were carried out and re shown in Fig. 10 and Tables 5 and 6. The XPS survey spectra exhibited prominent peaks which were C1 s, S2p, O1 s and K2p, and consequently the high-resolution XPS measurements were configured to include these elements. Table 5 summarizes the elemental compositions (at%) of the samples over the sampling depth of S atomic layers from the surface. As shown in Table 5, the relative percentage of the S atoms of exhausted WSBAC is higher than of fresh WSBAC. In order to further clarify the productions over exhausted WSBAC and exhausted WSBAC, Table 6 and Fig. 10 show the relevant detailed S2p XPS spectra of the fresh and exhausted WSBAC. Deconvolution of the S2p spectra gives three individual component groups that represent the sulfur/S (164.0 eV), RSOR (165.1 eV) and the sulfate/SO<sub>4</sub><sup>2-</sup> (168.8 eV). The contents of sulfur/S, RSOR and sulfate/SO<sub>4</sub><sup>2-</sup> on the exhausted WSBAC were higher than those of fresh WSBAC. Therefore, the products may be sulfur/S, sulfate and RSOR.

## Conclusion

By investigating the influences of different preparation conditions on the simultaneous removal of CS<sub>2</sub>, COS and H<sub>2</sub>S, the results showed that the WSBAC carbonized at 600 °C, then activated with 0.5 times KOH at 700 °C, had the

highest sulfur capacity (52.67 mgS/g<sub>WSBAC</sub>). The carbonization temperature has a great influence on the formation of the initial pores, and too high or too low carbonization temperature will influence the micropores and the total pore volume. WSBAC activated by KOH showed a high specific surface area. And WSBAC activated by 0.5 times of KOH has a greater pore volume with the radius of 0.3–1.8 nm. With the increasing of the activation temperature, the activation process can obtain enough energy, and large numbers of microporous can be produced at this stage. However, when the activation temperature is too high, the micropores could be converted to mesoporous, which led to the removal efficiency of CS<sub>2</sub>, COS and H<sub>2</sub>S being decreased. The XPS results showed that most of the products on the exhausted WSBAC were S/SO<sub>4</sub><sup>2-</sup> species which accumulated on the WSBAC's surface and had a negative effect on the adsorption activity.

**Acknowledgements** This work was supported by the National Natural Science Foundation of China (51408282, 21667015); China Scholarship Council (201508530017, 201608530169 and 201608740011) and the Analysis and Testing Foundation of Kunming University of Science and Technology.

## References

1. T. Toops, M. Crocker, *Appl. Catal. B Environ.* **82**, 199 (2008)
2. D.E. Sparks, T. Morgan, P.M. Patterson, S.A. Tackett, E. Morris, M. Crocker, *Appl. Catal. B Environ.* **82**, 190 (2008)
3. S.Z. Zhao, H.H. Yi, X.L. Tang, F.Y. Gao, Q.J. Yu, Y.S. Zhou, J.E. Wang, Y.H. Huang, Z.Y. Yang, *Ultrason. Sonochem.* **32**, 336 (2016)
4. J. Qiu, P. Ning, X.Q. Wang, K. Li, W. Liu, W. Chen, L.L. Wang, *Front. Environ. Sci. Eng.* **10**, 11 (2016)
5. X.Q. Wang, Y.X. Ma, P. Ning, J. Qiu, X.G. Ren, Z.Y. Li, W. Chen, W. Liu, *Adsorpt. J. Int. Adsorpt. Soc.* **20**, 623 (2014)
6. S.Z. Zhao, H.H. Yi, X.L. Tang, C.Y. Song, *Chem. Eng. J.* **226**, 161 (2013)
7. H. Wang, H. Yi, P. Ning, X. Tang, L. Yu, D. He, S. Zhao, *Chem. Eng. J.* **166**, 99 (2011)
8. P. Regmia, J.L.G. Moscosoa, S. Kumara, X. Caob, J. Maob, G. Schafrana, *J. Environ. Manag.* **17**, 61 (2012)
9. J. Zhang, L. Fan, C. Luo, P. He, *J. Environ. Sci.* **26**, 390 (2014)
10. C. Pan, L. Ye, J. Wang, L. Bao, Y. Que, *Chem. Res. Chin. Univ.* **29**, 941 (2013)
11. Y. Yegiazarov, J. Clark, L. Potapova, V. Radkevich, V. Yatsimirsky, D. Brunel, *Catal. Today* **102**, 242 (2005)
12. C. Huang, C. Chen, S. Chu, *J. Hazard. Mater.* **136**, 866 (2006)
13. Y. Lee, W. Park, J. Choung, D. Choi, *Environ. Sci. Technol.* **36**, 1086 (2002)
14. T. Chen, Z. Zhou, S. Xu, H. Wang, W. Lu, *Bioresour. Technol.* **190**, 388 (2015)
15. Q.F. Yu, M. Li, X. Ji, Y. Qiu, Y.T. Zhu, C.B. Leng, J. Wuhan, *Univ. Technol. Mat. Sci. Ed.* **31**, 260 (2016)
16. A.M. Stephan, T.P. Kumar, R. Ramesh, S. Thomas, S.K. Jeong, K.S. Nahm, *Mater. Sci. Eng. A* **430**, 132 (2006)
17. X. Song, P. Ning, C. Wang, K. Li, L. Tang, X. Sun, H. Ruan, *Chem. Eng. J.* **314**, 418 (2017)
18. K. Li, X. Song, P. Ning, H.H. Yi, X.L. Tang, C. Wang, *Energy Technol.* **3**, 136 (2015)
19. G. Tian, W. Wang, B. Mu, Y. Kang, A. Wang, *J. Taiwan Inst. Chem. Eng.* **50**, 252 (2015)
20. O. Ioannidou, A. Zabaniotou, *Renew. Sustain. Energy Rev.* **11**, 1966 (2007)
21. A. Jain, R. Balasubramanian, M.P. Srinivasan, *Chem. Eng. J.* **283**, 789 (2016)
22. S.M. Yakout, G.S. El-Deen, *Arab. J. Chem.* **9**, S1155 (2016)
23. Y. Xiao, C. Long, M. Zheng, H. Dong, B.U. Lei, H. Zhang, Y. Liu, *Chin. Chem. Lett.* **25**, 865 (2014)
24. S. Shahkarami, R. Azargohar, A.K. Dalai, J. Soltan, *J. Environ. Sci.* **34**, 68 (2015)
25. M.A. Lillo-Ródenas, D. Cazorla-Amorós, A. Linares-Solano, *Carbon* **41**, 267 (2003)
26. K. Labus, S. Gryglewicz, J. Machnikowski, *Fuel* **118**, 9 (2014)



27. J. Guo, Y. Luo, A.C. Lua, R. Chia, Y. Chen, X. Baoa, S. Xiang, *Carbon* **45**, 330 (2007)
28. K.Y. Foo, B.H. Hameed, *Bioresour. Technol.* **102**, 9814 (2011)
29. J.M. Ramos-Fernandez, M. Martinez-Escandell, F. Rodriguez-Reinoso, *Carbon* **46**, 384 (2008)